Journal of Hazardous Materials 205–206 (2012) 111–117

Contents lists available at SciVerse ScienceDirect

Journal of Hazardous Materials

journal homepage: www.elsevier.com/locate/jhazmat

Chromium (VI) and zinc (II) waste water co-treatment by forming layered double hydroxides: Mechanism discussion via two different processes and application in real plating water

Jia Zhang, Yang Li, Jizhi Zhou, Dan Chen, Guangren Qian*

School of Environmental and Chemical Engineering, Shanghai University, Shanghai 200072, PR China

ARTICLE INFO

Article history:
Received 18 September 2011
Received in revised form
15 December 2011
Accepted 15 December 2011
Available online 23 December 2011

Keywords:
Chromium (VI)
Zinc (II)
Layered double hydroxide (LDH)
Plating water

ABSTRACT

Two processes, adsorption after synthesis (AAS) and adsorption during synthesis (ADS) were compared in CrO_4^{2-} and Zn^{2+}/CrO_4^{2-} removal. Kinetic results showed that ADS was a better method than AAS, since Cr content was 0.65/0.81 mmol/g in Cr-ADS/ZnCr-ADS, but it was only 0.37/0.56 mmol/g in Cr-AAS/ZnCr-AAS. Then, a low-cost mixture was proposed to function as ADS raw materials in treating real plating waters. This mixture first got an isothermal saturation of 1.1 mmol/g in simulated CrO_4^{2-} water. When Zn^{2+} was co-treated, it was increased to 1.3 mmol/g. At the same time, a Zn^{2+} removal of 1.5 mmol/g was attained. Furthermore, real plating water co-treatment reached equilibrium in 6 h and obtained 1.4/0.9 mmol/g for Zn^{2+}/CrO_4^{2-}, respectively. According to XRD analysis, this co-treatment enhancement resulted from the formation of Zn and Cr contained layered double hydroxide.

1. Introduction

Metal-plating industry created large volumes of wastewater containing toxic metal ions such as Cd, Cu, Pb, Ni, Cr, and Zn ions [1,2]. All these substances are highly toxic and have been regulated by countries worldwide. Among them, CrO_4^{2-} and Zn^{2+} are typical anionic and cationic. CrO_4^{2-} is a highly hazardous material, being a mutagen and a potential carcinogen [3,4]. Greatly extra amount of Zn^{2+} in the environment may be very harmful because of its possibility of leading to irritability, lung disorders and even cancer [5]. Therefore, CrO_4^{2-} and Zn^{2+} effluents must be properly treated so as not to cause more damage to the environment. Recently, adsorption of CrO_4^{2-} or Zn^{2+} with a suitable adsorbent is widely studied [6–8]. However, since CrO_4^{2-} and Zn^{2+} were anionic and cationic, respectively, their co-treatment was seldom investigated.

Many adsorbents have been developed and studied on the adsorption characteristics towards specific contaminants. For example, CrO_4^{2-} can be adsorbed on materials, such as active carbons, anion exchange resins, natural fibers, biomass, various inorganic materials and inorganic nanoparticles [9–12]. Several kinds of environmental friendly materials have been observed to have high adsorption capacity for Zn^{2+} [13–15]. Among these choices, active carbons and anion exchange resins always result well CrO_4^{2-} removal efficiency. However, the production of active carbon is usually high energy cost (generally > 600 °C) [9]. Anion exchange resins are also costly in production. Other natural fibers and biomass are easily obtained but usually only have relative low removal amounts on CrO_4^{2-}. Compared with these methods, layered double hydroxides materials can be synthesized by low cost materials. Furthermore, they can take up CrO_4^{2-} in the interlayer with strong electrostatic interactions, showing a better adsorption property for CrO_4^{2-} removal [12,16,17]. Although layered double hydroxide is anion exchange clay and not usually researched on cation pollution removal, such as Zn^{2+}. However, Zn^{2+} is an ordinary component of layered double hydroxides [18,19], ordinarily but significantly, promising a possibility of Zn^{2+} and CrO_4^{2-} co-treatment.

Layered double hydroxides (LDHs) are a family of anionic clay materials. They can chemically be expressed as a general formula of $[M_{1-x}^{2+}M_x^{3+}(OH)_2](A^{n-})_{x/n}\cdot yH_2O$ [20–22], where M^{2+} and M^{3+} are any divalent (for example Zn^{2+}) and trivalent cations. A^{n-} is an exchangeable interlayer anion (for example CrO_4^{2-}). The most important property of LDHs is the high anion exchange capacity, promising the high removal efficiency of anionic contaminants [23–25]. As a matter of fact, LDHs have been noted to adsorb CrO_4^{2-} in a reasonably high amount both in batch and column experiments [16,26]. It is our hypothesis that merging CrO_4^{2-} and Zn^{2+} treatment is possible and applicable.

Therefore, this work is aimed to prove the possibility and applicability of CrO_4^{2-}/Zn^{2+} co-treatment via layered double hydroxides both in simulated and real waste water. To this end, we first

* Corresponding author. Tel.: +86 21 66137758; fax: +86 21 66137758.
E-mail addresses: grqian@mail.shu.edu.cn, grqian@shu.edu.cn, grqian@staff.shu.edu.cn (G. Qian).

0304-3894/$ – see front matter © 2012 Elsevier B.V. All rights reserved.
doi:10.1016/j.jhazmat.2011.12.040

compared CrO_4^{2-} and Zn^{2+} adsorption by two different methods. (1) adsorption after synthesis (AAS); (2) adsorption during synthesis (ADS). Kinetic and isothermal adsorptions were carefully finished and mechanisms were investigated. Then, according to these results, a novel method via batch experiments was proposed to treat real CrO_4^{2-} and Zn^{2+} plating water.

2. Experimental

2.1. Adsorption after the synthesis of LDHs

CaAl-Cl LDHs (Friedel's salt) was prepared by a coprecipitation method, as described elsewhere [27]. In general, two solutions were first prepared, one contained 1 mol/L $CaCl_2$ and 0.5 mol/L $AlCl_3$, and another one contained 1.5 mol/L NaOH. Then they were mixed at a volume ratio of 1:2 under vigorous stirring with a magnetic stirrer. The synthesis of Friedel' salt was performed under nitrogen protection in order to prevent the probable influence of CO_2. All reagents were of reagent grade quality and were purchased from Sinopharm Chemical Reagent Co. Ltd. After aging overnight at room temperature, the resultant slurry was collected and washed by distilled water during filtration. Finally, it was dried at 105 °C for 24 h. The obtained sample was ground and stored in a desiccator for further use.

Formula of this synthesized Friedel's salt was then analyzed as $Ca_{3.8}Al_2(OH)_{11.6}Cl_2(H_2O)_{5.8}$ by inductively coupled plasma optical emission spectrometer (ICP-AES). In the end, 0.2 g of this solid was used to adsorb 50 ml of 10 mmol/L CrO_4^{2-} or 28.5 mmol/L Zn^{2+} + 10 mmol/L CrO_4^{2-} contaminated water. We call this process as adsorption after the synthesis of LDHs (defined simply as AAS).

2.2. Adsorption during the synthesis of LDHs

In the former AAS method, if 0.2 g input of Friedel's salt were totally dissolved in the targeted 50 ml waste water, concentrations of Ca^{2+}, Al^{3+} and OH^- would be about 28.5, 14.3 and 85.5 mmol/L, respectively. According to these, two solutions were mixed to create a process of LDHs synthesis and pollution adsorption at the same time. They were one salt solution containing 57 mmol/L Ca^{2+} and 28.5 mmol/L Al^{3+}, another CrO_4^{2-} contaminated water with 171 mmol/L NaOH. When Zn^{2+} was co-treated, 57 mmol/L Zn^{2+} would be added in the former salt solution. 25 ml liquid from each solution were then mixed together for LDHs synthesis and ions adsorption. We call this process as adsorption during the synthesis of LDHs (distinctly defined as ADS).

2.3. Application of adsorption during the synthesis

After all, input of pure reagent is not as economic as low cost materials, such as cement. Considering real application, cement was utilized to replace salt solution, since it could function as a source of Al. It was identified that the cement used in our work contained about 50% Al_2O_3. As a result, cement and $Ca(OH)_2$ were mixed thoroughly with a weight ratio of 45:31 to create a Ca/Al mole ratio of about 2. The resulted mixture was kept for further application of adsorption during the synthesis to treat real Zn^{2+} (20 mmol/L)/CrO_4^{2-} (14 mmol/L) plating water.

2.4. Characterization

Ca^{2+}, Al^{3+}, Zn^{2+} and CrO_4^{2-} concentrations before and after adsorption in all experiments were determined by inductively coupled plasma optical emission spectrometer (ICP-AES). The evolved solids were washed by distilled water after filtration. They were dried at 100 °C for further components and XRD analysis.

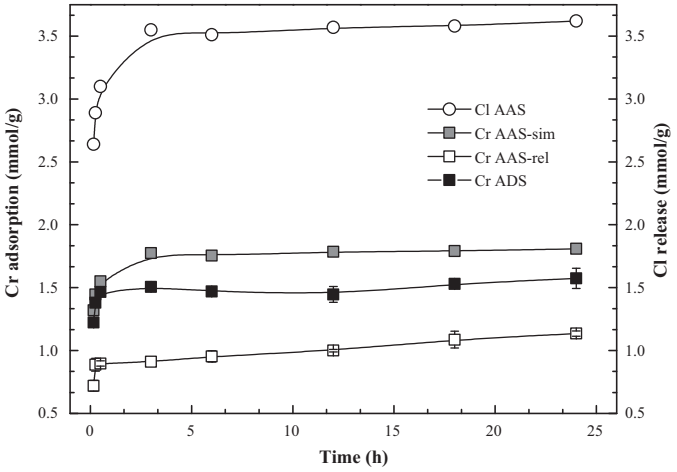

Fig. 1. Cr(VI) removal by adsorption after synthesis (AAS) and adsorption during synthesis (ADS); Cr AAS-rel is the real Cr(VI) adsorption data. Cr AAS-sim is theoretical Cr(VI) adsorption amount according to chlorine release.

Components analysis was applied to determine the exact metal ratio in dried solids. In general, 0.05 g was dissolved in diluted acid before concentrations being detected by ICP-AES. Chloride in solutions was titrated with silver nitrate. The XRD patterns of all obtained compounds were recorded in an XRD DLMAX-2550 (Rigaku Co.) using Cu K_α radiation (λ = 0.15418 nm) from 5 to 80° at a scanning rate of 8°/min.

3. Results and discussion

3.1. CrO_4^{2-} removal by AAS and ADS

Fig. 1 compares adsorption after synthesis (AAS) with adsorption during synthesis (ADS) on removal process. It is obvious that ADS obtained a better removal effect than AAS, since the former reached an adsorption amount of 1.5 mmol/g, while the latter only got a 1.1 mmol/g. However, they were neither bigger than the theoretical 1.8 mmol/g according to the adsorbent weight. Still, both methods attained equilibrium at about 3 h.

In the AAS method, Cl^- released from Friedel's salt into solution step by step and maintained at about 3.6 mmol/g after 3 h. Similarly, the CrO_4^{2-} removal got equilibrium at the same time, exhibiting a possible anion exchange process. In addition, CrO_4^{2-} has a higher inclination into the LDH interlayer than Cl^- [28]. In this work, it was likely that most of Cl^- was exchanged by other anions, such as CrO_4^{2-}, since there was theoretically 3.6 mmol/g Cl^- in the Friedel's salt according to the synthesized formula. If Cl^- was totally exchanged by CrO_4^{2-}, CrO_4^{2-} removal amount would be half of Cl^- release amount, which was also depicted in Fig. 1(Cr AAS-sim). It was clear that Cr AAS-rel was lower than Cr AAS-sim for about 1 mmol/g. There were two main reasons. Firstly, other anions (CO_3^{2-}, HCO_3^-, etc.) probably entered into the interlayer [28]. Secondly, part of Friedel's salt dissolved into the solution. As a result, the real amount was much smaller, and AAS method got a final removal of 1.1 mmol/g.

As for ADS method, Cl^- was kept at almost 0.11 mol/L during the whole process. Since Cl^- was 0.21 mol/L in the origin Ca^{2+} and Al^{3+} solution by titration, the total Cl^- input would be 0.11 mol/L after the mixture of Ca^{2+}/Al^{3+} and NaOH solutions. Considering this, Cl^- seemed to play no role in exchanging CrO_4^{2-} in ADS. On the other hand, CrO_4^{2-} removal amount reached balance at 1.5 mmol/g within the first 0.5 h, faster than AAS method which attained balance at about 3 h. Although it was still a little lower than the theoretical 1.8 mmol/g, it was much bigger than the 1.1 mmol/g

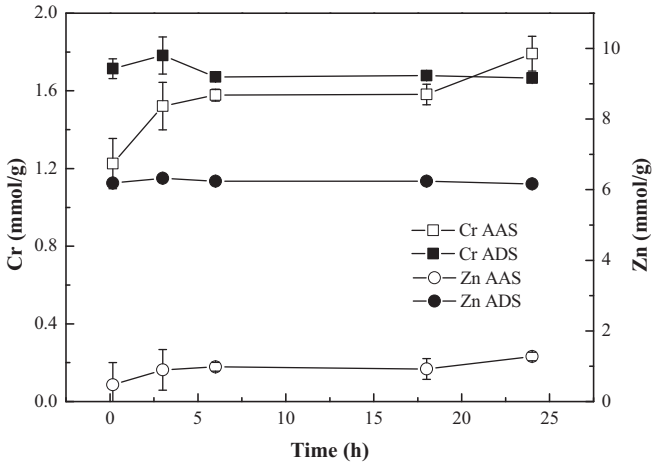

Fig. 2. Zn^{2+} and CrO_4^{2-} co-adsorption by AAS and ADS.

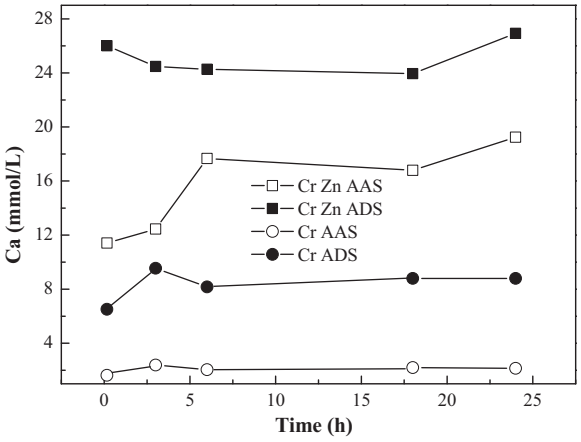

Fig. 3. Ca^{2+} release in CrO_4^{2-} and Zn^{2+}/CrO_4^{2-} adsorption via AAS and ADS.

in AAS. Three main reasons accounted for these. (1) It took time for CrO_4^{2-} to exchange interlayer Cl^- in Friedel's salt, but it almost took no time for mixture of two solutions. As a result, ADS is faster to reach equilibrium. (2) During the synthesis of Friedel's salt, some interlayer spaces were inevitably occupied by anions such as CO_3^{2-} [28]. As a result, AAS had a lowered exchangeable amount than ADS. (3) Some of the synthesized Friedel's salt was dissolved into Ca^{2+} and $Al(OH)_4^-$ to reach dissolution–deposition equilibrium [29]. However, much more of them were deposited into $CaCO_3$ and $Al(OH)_3$ in AAS than ADS. This was another reason why ADS had a higher adsorption capacity.

3.2. CrO_4^{2-}, Zn^{2+} co-removal by AAS and ADS

In order to further understand AAS and ADS, CrO_4^{2-} and Zn^{2+} adsorption by these two methods were researched. Their adsorptions along time are carefully compared in Fig. 2. In general, AAS and ADS obtained a similar final CrO_4^{2-} adsorption amount of 1.6 and 1.7 mmol/g. However, final Zn^{2+} amount was 1.2 and 6.3 mmol/g for AAS and ADS, respectively, because AAS and ADS removed Zn^{2+} by different mechanism. Generally, it is proposed that AAS removed Zn^{2+} by Ca^{2+} replacement but Ca^{2+} in Friedel's salt could only be partially exchanged. By comparison, ADS removed Zn^{2+} by forming LDH with Al^{3+} and CrO_4^{2-}. As a result, ADS has a higher removal of Zn^{2+} over AAS.

In AAS, CrO_4^{2-} adsorption amount climbed from 1.2 to around 1.6 mmol/g in the end. As for Zn^{2+}, it kept almost the same trend as CrO_4^{2-}. It got a removal of 1.0 mmol/L at the initial period, and then increased slowly to 1.2 mmol/g. Fig. 3 depicts Ca^{2+} release during the adsorption. It was obvious that Ca^{2+} started to dissolve from Friedel's salt at the same time with the CrO_4^{2-} and Zn^{2+} adsorption. Specifically, its dissolution increased from 11.4 to 17.7 mmol/L in the first 6 h, and reached 19.2 mmol/L in the following 18 h.

Unlike AAS, ADS went on a different way. As Fig. 2 shows, at the first contact, CrO_4^{2-} adsorption almost reached equilibrium and gained a capacity of 1.7 mmol/g. Ca^{2+} concentration in the liquid phase and Zn^{2+} adsorption held a similar changing rule. They kept at about 25 mmol/L and 6.2 mmol/g, respectively, during the entire procedure. AAS needed longer time to reach equilibrium than ADS, this proved our assumption that AAS removed Zn^{2+} and CrO_4^{2-} by exchange with Ca^{2+} and Cl^-, but AAS removed these pollutants by forming LDH as soon as the two solutions are mixed. On the other hand, Ca^{2+} release in ADS was bigger than that of AAS, showing that Ca^{2+} was only partially replaced by Zn^{2+} in AAS.

Fig. 3 also compares Ca^{2+} releases of AAS and ADS in CrO_4^{2-} treatment. In AAS and ADS, when Friedel's salt was used to adsorb Zn^{2+} synchronously with CrO_4^{2-}, Ca^{2+} release was much higher than the case treating CrO_4^{2-} only. While, CrO_4^{2-} treating capacity was 1.7 mmol/g in Zn^{2+} simultaneous treating, a little bigger than 1.6 mmol/g in mere CrO_4^{2-} removal. By comparison, in AAS, it was obvious that Zn^{2+} played a main role in the increase of CrO_4^{2-} adsorption amount from 1.3 to 1.7 mmol/g, and as a result, final adsorption amount in AAS was almost the same as that in ADS.

3.3. Removal mechanisms of AAS and ADS

In order to analyze the removal mechanisms during AAS and ADS, solid samples after 0.16 h and 24 h were collected and dried for XRD analysis. These solid included both CrO_4^{2-} and CrO_4^{2-}/Zn^{2+} adsorption. In addition, the origin synthesized Friedel's salt was also scanned. All these XRDs are compared in Figs. 4 and 5, almost all of them showed a process of forming LDH patterns.

Fig. 4 compares AAS and ADS process in CrO_4^{2-} adsorption. They both exhibited a process of forming LDHs. The synthesized Friedel's salt fits well with the reported one (JCPDS No. 78-1219) [27,29]. For AAS, it seemed that most of Friedel's salt had dissolved at the first adsorption period, since the solid sample almost showed a mere

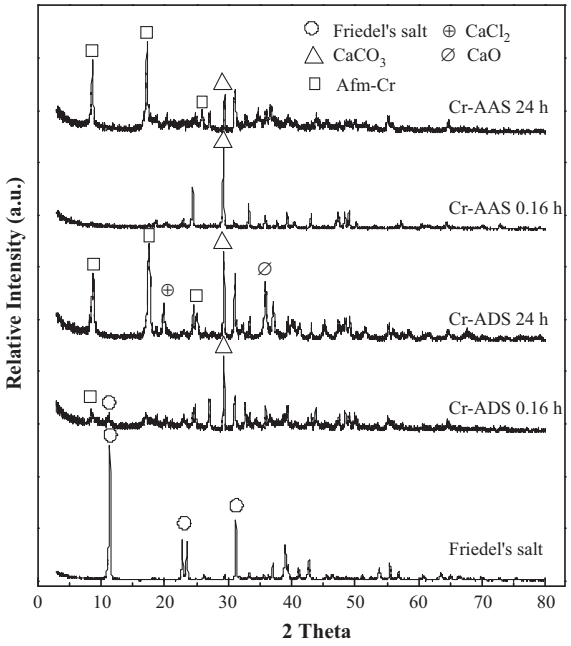

Fig. 4. XRD in Cr(VI) treatment by AAS and ADS.

Table 1
Final metal contents and M_{II}/M_{III} after adsorption.

Sample	Al (mmol/g)	Ca (mmol/g)	Zn (mmol/g)	Cr (mmol/g)	M_{II}/M_{III}
Cr-ADS 0.16 h	0.80	1.67	–	0.52	2.09
Cr-ADS 6 h	0.81	1.52	–	0.49	1.88
Cr-ADS 24 h	0.97	2.05	–	0.65	2.11
Cr-AAS 0.16 h	1.24	2.23	–	0.37	1.80
Cr-AAS 6 h	0.83	1.61	–	0.37	1.93
Cr-AAS 24 h	1.24	2.23	–	0.37	1.80
ZnCr-ADS 0.16 h	1.58	0.11	2.18	0.78	1.45
ZnCr-ADS 6 h	1.40	0.13	2.06	0.72	1.57
ZnCr-ADS 24 h	1.21	0.13	2.27	0.81	1.99
ZnCr-AAS 0.16 h	1.06	1.13	0.85	0.27	1.86
ZnCr-AAS 6 h	1.13	0.83	0.81	0.42	1.45
ZnCr-AAS 24 h	1.58	0.64	1.55	0.56	1.39

calcium carbonate phase after 0.16 h contacting with CrO_4^{2-} simulated waste water. However, after 24 h, the corresponding solid sample contained mainly a phase like calcium aluminum oxide sulfate hydrate ($Ca_4Al_2SO_4 12OH{\cdot}10H_2O$, JCPDS No. 44-0602) or called AFm [30], which is also a kind of layered clay. Since SO_4^{2-} did not exist in the solution largely, it was considered to be a phase of chromate-AFm (AFm–Cr) [31]. The whole adsorption process is concluded as old LDH phase dissolution and new one formation.

Similarly, ADS exhibited a process of AFm–Cr formation. At the first step, the solid phase after 0.16 h appeared two main components. They were Friedel's salt and AFm phase. However, after 24 h, the main peaks turned out to be dominated AFm–Cr. In other words, AFm–Cr phase grew during the whole period while Friedel's salt just flashed at the first time. AFm–Cr seemed to be more stable than Friedel's salt, since the latter almost totally disappeared after equilibrium. This was also observed in case of AAS. In addition, there was $CaCO_3$, $CaCl_2$ and CaO in the solid phases. Since Ca^{2+} existed in this system, it was inevitably formed. After all, regardless of AAS or ADS, after 24 h's equilibrium, the final Cr-solidified phase was AFm–Cr.

Fig. 5 compares AAS and ADS processes in CrO_4^{2-} and Zn^{2+} adsorption. The left part showed the whole patterns and the right one focused on the main peak around 11–12 θ. In general, in treating CrO_4^{2-} and Zn^{2+} waste water, the main final phase was ZnAl—CrO_4^{2-} LDH. In ZnCr-AAS method, when being input into the liquid, Friedel's salt began to dissolve in the solution. At the same time, a ZnAl-LDH phase started to grow, and finally became the main solid component after 24 h. During this process, some Al_2O_3 appeared because of the formed $Al(OH)_3$ during Friedel's salt dissolution. After all, we called the main phase ZnAl-LDH_{AAS}.

Differently, ZnCr-ADS 0.16 h and 24 h (Fig. 5) were almost the same with a slight difference, and the main peaks were attributed to the expected ZnAl-LDH. It formed easily as the corresponding peaks appeared at the first 0.16 h. However, it was called ZnAl-LDH_{ADS} for distinguish. But nevertheless AAS or ADS, CrO_4^{2-} and Zn^{2+} adsorption resulted a final ZnAl-LDH phase.

In order to further review the adsorption and formation periods, the solid samples were in step analyzed to check their metal components. Possible formulas and Cr occupation (mmol/g) were all listed in Table 1. Table 2 listed some LDH physical parameters in CrO_4^{2-} and Zn^{2+} adsorption.

In CrO_4^{2-} AAS adsorption, Al, Ca, Cr contents and M_{II}/M_{III} were almost kept the same from 0.16 to 24 h. Since the origin $M_{II}/M_{III} = 1.90$, there seemed to be a slight decrease as the final ratio was 1.80. However, Cr content was 0.37 mmol/g generally, proving our hypothesis that Friedel's salt's adsorption completed

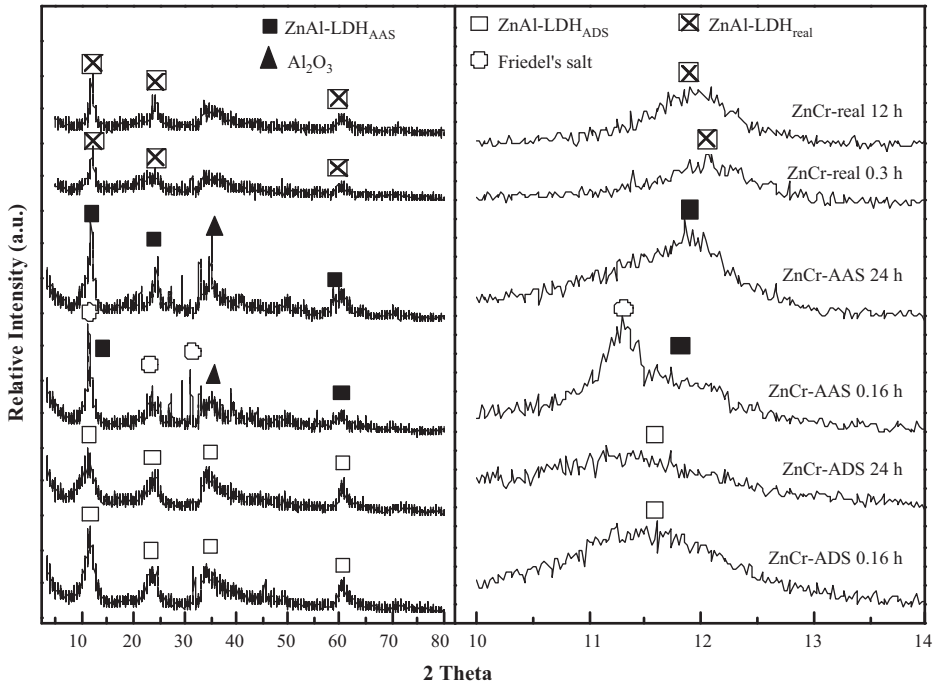

Fig. 5. XRD in Zn^{2+} and CrO_4^{2-} treatment by AAS and ADS. The right figure was extracted from the left from 10 to 14 degree.

Table 2
Physical parameters of Friedel's salt and the obtained products.

Sample	*a* (nm)	*c* (nm)
Friedel's salt synthesis	0.57	1.55
ZnCr-ADS 0.16 h	0.31	2.30
ZnCr-ADS 24 h	0.31	2.38
ZnCr-AAS 0.16 h	0.57/0.30	1.56/2.24
ZnCr-AAS 24 h	0.31	2.24
ZnCr-real 0.3 h	0.31	2.20
ZnCr-real 12 h	0.31	2.22

at a very fast speed. Similarly in CrO_4^{2-} ADS adsorption, M_{II}/M_{III} almost maintained around 2. Furthermore, final CrO_4^{2-} content was 0.65 mmol/g, much bigger than that in CrO_4^{2-} AAS adsorption. All after all, M_{II}/M_{III} in all samples changed around 1.90. This showed that the resulted solid was more inclined to form the origin metal ratio material. Interestingly in both cases, there were differences at 6 h in metal contents and ratios. We think it to be an intermediate unstable period. In addition, in Table 1, Cr/Zn content stood for Cr/Zn relative percentage in the formed solid after adsorption. By contrast, in Fig. 1 and 2, Cr/Zn removal amount was calculated from Cr/Zn concentration decrease by per gram of the origin adsorbent. However, the formed solid was heavier than the origin one. As a result, Cr and Zn contents in Table 1 were smaller than removal mount in Figs. 1 and 2.

In Zn^{2+} and CrO_4^{2-} adsorption system, mechanism seemed to be different. In AAS, Ca^{2+} was replaced by Zn^{2+} step by step from the solid phase. The Ca^{2+} content was 1.13 mmol/g at 0.16 h, and it decreased to 0.83 and 0.64 mmol/g, respectively in 6 and 24 h. At the same time, Cr grew from 0.27 to 0.42 and 0.56 mmol/g. Although enough Zn^{2+} was pretended to replace Ca^{2+}, there was still Ca left in the solid phase. According to the XRD analyze, it seemed to be in the form of $CaCO_3$. While, at 0.16 h, there was still some little Friedel's phase formed. In contrast, Zn^{2+} and CrO_4^{2-} contents grew bigger and bigger, and at last, they reached 1.55 and 0.56 mmol/g, respectively. While, in this case, M_{II}/M_{III} went down from 1.90 to 1.86, 1.45 and finally 1.39. This meant that Ca^{2+} release amount was much bigger than Zn^{2+} removal amount in Friedel's salt. As a result, Al contents in the solid phase increased from 1.06 to 1.13 and 1.58 mmol/g. Furthermore, $Al(OH)_3$ seemed to form during these processes, because there were peaks of Al_2O_3 around 35 θ in XRD (Fig. 5) and the resulted M_{II}/M_{III} was smaller than the reasonable 2–4 for LDHs [28], which means an over amount of Al.

In Zn^{2+} and CrO_4^{2-} ADS adsorption, Ca, Zn and Cr contents maintained at 0.13, 2.27 and 0.81 mmol/g during the adsorption process. As for the Al content, it decreased slightly from 1.58 to 1.40 and 1.21 mmol/g. As a result, M_{II}/M_{III} changed from 1.45 to 1.57 and 1.99. It was interesting that Cr amount (mmol/g) was almost constant in Cr-AAS, Cr-ADS and ZnCr-ADS because they were fast processes. However, Cr amount went up in ZnCr-AAS because the increase of Zn amount increased the exchangeable amount of Cr in Friedel's salt. If we do not add Ca^{2+} and left Zn^{2+} to participate in this method, the main phase would still be ZnAl—CrO_4^{2-} LDH, since XRD of the solid was mainly ZnAl—CrO_4^{2-} and large amount of Ca^{2+} remained in solution. On the other condition, if Zn^{2+} concentration was low in target waste water, it was necessary to add Ca^{2+} to obtain an acceptable CrO_4^{2-} removal amount.

In summary, Zn and Cr removal amounts of ADS were always bigger than those of AAS both in Cr and ZnCr adsorption. From this point of view, we thought ADS adsorption to be a better choice. Since the synthesis period was omitted, whole management was also saved. There were several reasons. (1) The synthesized sorbent was not totally pure and the dissolution loss was great during adsorption. (2) In situ synthesis seemed to benefit the distribution of metal species and resulted in a reasonable content ratio, since the ADS cases always owned one around 2.00 and AAS ones were relative lower. In addition, physical parameters also depicted the same results. As Table 2 shows, *c* in AAS was 2.244 and 2.238 (nm), while it was 2.304 and 2.376 (nm) in ADS. This indicated that the average interlayer space was supported much bigger in ADS than in AAS. In other words, more CrO_4^{2-} anions went into the interlayer, resulting in a bigger adsorption amount.

3.4. Application of ADS in CrO_4^{2-} and Zn^{2+} co-removal

In order to investigate the real effect in applying ADS, a mixture (raw materials) containing cement and $Ca(OH)_2$ was proposed to substitute Ca/Al solution.

Fig. 6 shows CrO_4^{2-} and CrO_4^{2-}/Zn^{2+} adsorption isothermal. In Fig. 6A, CrO_4^{2-} adsorption, Ca^{2+} and Al^{3+} dissolution amount showed different trends. With the increase of initial CrO_4^{2-} concentration, CrO_4^{2-} adsorption amount increased and reached a final saturation adsorption amount of about 1.1 mmol/g. Similarly, Ca^{2+} in solution increased from 3.5 to 4.5 mmol/L during the whole period. In contrary, Al^{3+} concentration first decreased, then kept a constant value and at last increased. When initial CrO_4^{2-} concentration < 3 mmol/L, the removal was 0.7 mmol/g CrO_4^{2-}, about two-third of the final amount. At the same time, Al^{3+} decreased together with a slight increase in Ca^{2+}. It was proposed that with the increase of initial CrO_4^{2-} concentration, more and more Al^{3+} was utilized in forming AFm–Cr. As a result, Al^{3+} concentration almost attained 0.15 mmol/L under an input of 3 mmol/L. When the initial concentration was between 3 and 8 mmol/L, Al^{3+} is kept at 0.15 mmol/L while CrO_4^{2-} adsorption amount climbed from 0.7 to equilibrium of 1.1 mmol/g. During this step, AFm–Cr occupied more and more parts in total AFm-A^{n-} phase (A^{n-} stand for CrO_4^{2-},

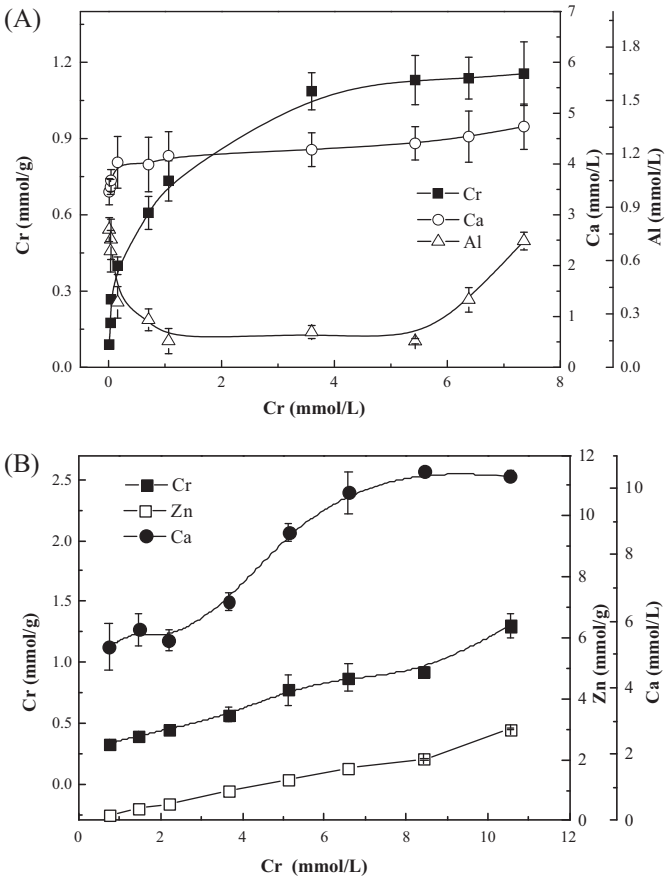

Fig. 6. ADS isothermals in application of treating real plating waste water (A) CrO_4^{2-}, (B) CrO_4^{2-}/Zn^{2+}.

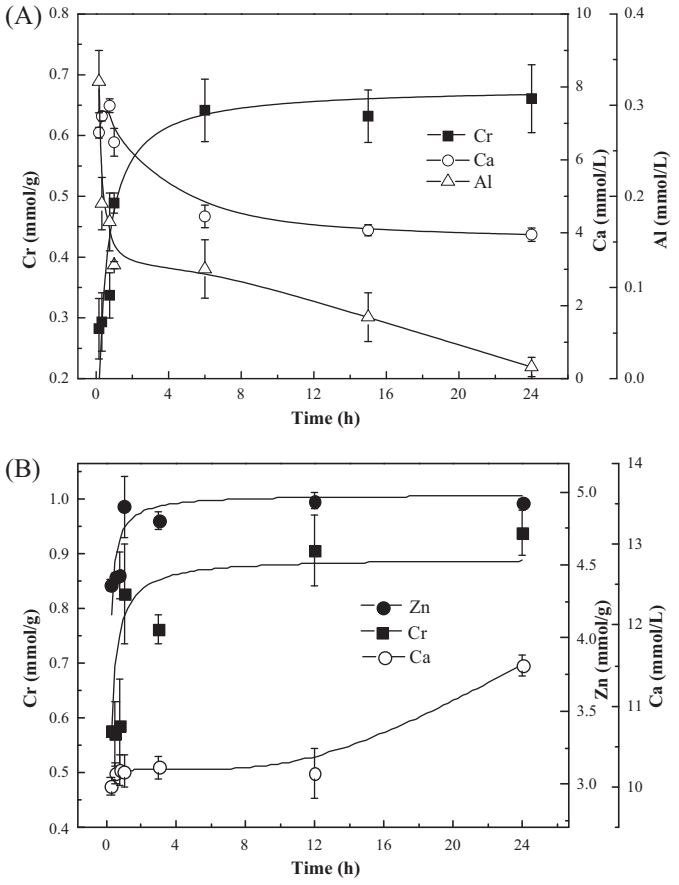

Fig. 7. ADS kinetics in application of treating real plating waste water (A) CrO_4^{2-}, (B) CrO_4^{2-}/Zn^{2+}.

OH^-, HCO_3^-, etc.). After this saturation point, the equilibrium point came. It was interesting that there was an increase in Al^{3+} with a step increase in initial CrO_4^{2-} concentration. Since CrO_4^{2-} adsorption amount went no down, this increase came from other AFm phase except for AFm–Cr. It seemed that an over level of CrO_4^{2-} created no more AFm–Cr but accelerated the dissolution of AFm-A^{n-} (A^{n-} stand for OH^-, HCO_3^-, etc.).

Fig. 6B shows Zn^{2+} and CrO_4^{2-} waste water co-treatment isothermal. With the increase of Zn^{2+}/CrO_4^{2-} initial concentration, Zn^{2+} and CrO_4^{2-} adsorption amount increased, together with an obvious increase in Ca^{2+} concentration. This Ca^{2+} increase came from Ca^{2+} substitution from the AFm–Cr by Zn^{2+}. As a result, ZnAl–Cr LDH came into formation. However, at a high level of Zn^{2+}/CrO_4^{2-} initial concentration, Ca^{2+} concentration stopped increase and maintained at 11 mmol/L. Since not all Ca^{2+} could be substituted, they might be left in the crystal LDH. From Fig. 6B, a good affinity of Zn^{2+} and CrO_4^{2-} removal trend could be observed. This indicated that LDH also formed at an acceptable affinity and ADS process could remove Zn^{2+} and CrO_4^{2-} at a satisfying efficiency. For example, when Zn^{2+} removal increased from 0.96 to 2.02 and 3.00 mmol/g, CrO_4^{2-} removal almost kept a same pace from 0.57 to 0.92 and 1.30 mmol/g, respectively. Furthermore, Al^{3+} dissolved little in each point, which differed from Fig. 6A. This was accounted to the existence of Zn^{2+}, which accelerated the formation of LDH, utilizing Al^{3+} effectively.

All after all, nevertheless CrO_4^{2-} or Zn^{2+}/CrO_4^{2-} system, our raw material could work at a high level in waste removal. In order to further testify this mixture, two real plating CrO_4^{2-} and Zn^{2+} waste water (about 14 and 20 mmol/L, respectively) were tested.

Fig. 7A depicts CrO_4^{2-} adsorption kinetic. The adsorption reached equilibrium fast at 6 h and attained an acceptable adsorption amount of 0.66 mmol/g. However, Ca^{2+} and Al^{3+} decreased all the time. From 0 to 6 h, Ca/Al decreased from 8/0.2 to 4/0.1 mmol/L in the solution. This decrease could be accounted for the adsorption of CrO_4^{2-} and the formation of AFm–Cr. After this period, Ca/Al went down, resulting from the formation of other AFm phase, for example, AFm-OH [32]. In addition, from 0.16 to 1 h, Ca^{2+} first dissolved then deposited. The dissolution came from the release of Ca^{2+} from raw materials. Although this release went on through the whole adsorption, the speed of deposit formation was obvious much faster, as a result, Ca^{2+} increased slightly at the first period, while decreased over the later time.

Fig. 7B compares Zn^{2+}/CrO_4^{2-} adsorption kinetic with solo CrO_4^{2-} adsorption (Fig. 7A). It got equilibrium at about 4 h both for Zn^{2+} and CrO_4^{2-}. All in all, they obtained adsorption amounts of 5 and 0.9 mmol/g, respectively. Its CrO_4^{2-} adsorption amount was bigger than that of Fig. 7A because of the existence of Zn^{2+}, and the resulting ZnAl–Cr LDH. However, although Ca^{2+} concentration little changed during this period, it increased from 3.0 to 3.7 mmol/L at the last adsorption period. It was proposed that Ca^{2+} in fact first included in the ZnAl–Cr LDH crystal. Since LDH always goes on a dissolution and deposition process, Ca^{2+} was released with the time going on. In addition, during the whole process, just like the Zn^{2+}/CrO_4^{2-} isothermal (Fig. 6B), Al^{3+} was little detected. Furthermore, XRDs of ZnCr-real 0.3 and 12 h in Fig. 5 exhibited obvious LDH pattern. Their physical parameters are listed in Table 2. ZnCr-real 0.3 h showed an interlayer *c* of 0.20 nm. Then, it increased to 2.22 nm, small but significant, showing the difference in adsorption amounts. As for *a*, there were little changes, both kept around 0.31 nm.

After all, these results testify the possibility of co-treatment of Zn^{2+} and CrO_4^{2-} waste water. Although the result solid was different from each other when the initial Zn^{2+}/CrO_4^{2-} waste differed, the adsorption amount was acceptable for the simulated CrO_4^{2-} or Zn^{2+}/CrO_4^{2-} adsorption.

4. Conclusion

In this work, CrO_4^{2-} or Zn^{2+}/CrO_4^{2-} waste water was investigated by two different removal methods: Adsorption after synthesis (AAS) and adsorption during synthesis (ADS). Kinetic results showed ADS a better way in waste treating, since it always attained a better adsorption amount. Specifically, AFm–Cr was the main solid phase in CrO_4^{2-} treatment, compared with ZnAl–Cr LDH in Zn^{2+}/CrO_4^{2-} system. Then, a low-cost raw material containing cement and $Ca(OH)_2$ was proposed to co-treat real Zn^{2+}/CrO_4^{2-} waste water via ADS. According to XRD analysis, the co-treated product was obvious ZnAl–Cr LDH. This work opened an opportunity for a co-treatment method of different heavy metal waste water, together with obtaining useful LDH products.

Acknowledgements

This project is financially supported by National Nature Science Foundation of China No. 20677037, No. 20877053, No. 21107067, National Major Science and Technology Program for Water Pollution Control and Treatment 2009ZX07106-01, 2008ZX0742-002 and Shanghai Leading Academic Discipline Project No. S30109.

References

[1] N. Adhoum, L. Monser, N. Bellakhal, J.E. Belgaied, Treatment of electroplating wastewater containing Cu^{2+}, Zn^{2+} and Cr(VI) by electrocoagulation, J. Hazard. Mater. 112 (2004) 207–213.
[2] I.A.H. Schneider, J. Rubio, Sorption of heavy metal ions by the nonliving biomass of freshwater macrophytes, Environ. Sci. Technol. 33 (1999) 2213–2217.

[3] H.Y. Shen, Y.G. Zhao, S.D. Pan, M.Q. Hu, Synthesis, characterization and properties of ethylenediamine-functionalized Fe_3O_4 magnetic polymers for removal of Cr(VI) in wastewater, J. Hazard. Mater. 182 (2010) 295–302.
[4] L.Z. Zhang, Z.H. Ai, Y. Cheng, J.R. Qiu, Efficient removal of Cr(VI) from aqueous solution with Fe@Fe_2O_3 core–shell nanowires, Environ. Sci. Technol. 42 (2008) 6955–6960.
[5] E.M. Cuerda-Correa, M.D. Gomez-Tamayo, A. Macias-Garcia, M.A.D. Diez, Adsorption of Zn(II) in aqueous solution by activated carbons prepared from evergreen oak (*Quercus rotundifolia* L.), J. Hazard. Mater. 153 (2008) 28–36.
[6] G. Furrer, U. Wingenfelder, C. Hansen, R. Schulin, Removal of heavy metals from mine waters by natural zeolites, Environ. Sci. Technol. 39 (2005) 4606–4613.
[7] I.M.C. Lo, T.Z. Liu, D.C.W. Tsang, Chromium(VI) reduction kinetics by zero-valent iron in moderately hard water with humic acid: iron dissolution and humic acid adsorption, Environ. Sci. Technol. 42 (2008) 2092–2098.
[8] H.P. He, P. Yuan, M.D. Fan, D. Yang, D. Liu, A.H. Yuan, J.X. Zhua, T.H. Chen, Montmorillonite-supported magnetite nanoparticles for the removal of hexavalent chromium [Cr(VI)] from aqueous solutions, J. Hazard. Mater. 166 (2009) 821–829.
[9] D. Mohan, C.U. Pittman, Activated carbons and low cost adsorbents for remediation of tri- and hexavalent chromium from water, J. Hazard. Mater. 137 (2006) 762–811.
[10] F. Gode, E. Pehlivan, Removal of Cr(VI) from aqueous solution by two Lewatit-anion exchange resins, J. Hazard. Mater. 119 (2005) 175–182.
[11] Y.M. Tzou, L.C. Hsu, S.L. Wang, Y.C. Lin, M.K. Wang, P.N. Chiang, J.C. Liu, W.H. Kuan, C.C. Chen, Cr(VI) removal on fungal biomass of Neurospora crassa: the importance of dissolved organic carbons derived from the biomass to Cr(VI) reduction, Environ. Sci. Technol. 44 (2010) 6202–6208.
[12] Y.J. Li, B.Y. Gao, T. Wu, D.J. Sun, X. Li, B. Wang, F.J. Lu, Hexavalent chromium removal from aqueous solution by adsorption on aluminum magnesium mixed hydroxide, Water Res. 43 (2009) 3067–3075.
[13] X.Y. Guo, S. Liang, Q.H. Tian, Adsorption of Pb^{2+} and Zn^{2+} from aqueous solutions by sulfured orange peel, Desalination 275 (2011) 212–216.
[14] D. Goyal, S.S. Ahluwalia, Microbial and plant derived biomass for removal of heavy metals from wastewater, Bioresour. Technol. 98 (2007) 2243–2257.
[15] H.D. Doan, V.B.H. Dang, T. Dang-Vu, A. Lohi, Equilibrium and kinetics of biosorption of cadmium(II) and copper(II) ions by wheat straw, Bioresour. Technol. 100 (2009) 211–219.
[16] G.R. Qian, Y.F. Xu, J. Zhang, Z. Ren, Z.P. Xu, Y.Y. Wu, Q. Liu, S.Z. Qiao, Effective Cr(VI) removal from simulated groundwater through the hydrotalcite-derived adsorbent, Ind. Eng. Chem. Res. 49 (2010) 2752–2758.
[17] V. Rives, D. Carriazo, M. del Arco, C. Martin, A comparative study between chloride and calcined carbonate hydrotalcites as adsorbents for Cr(VI), Appl. Clay Sci. 37 (2007) 231–239.
[18] A.M. Fogg, G.R. Williams, R. Chester, D. O'Hare, A novel family of layered double hydroxides – $[MAl_4(OH)_{12}](NO_3)_2{\cdot}H_2O$ (M = Co, Ni, Cu, Zn), J. Mater. Chem. 14 (2004) 2369–2371.
[19] A. Dias, A.C. Vieira, R.L. Moreira, Raman scattering and Fourier transform infrared spectroscopy of $Me_6Al_2(OH)_{16}Cl_2{\cdot}4H_2O$ (Me = Mg, Ni, Zn, Co, and Mn) and $Ca_2Al(OH)_6Cl{\cdot}2H_2O$ hydrotalcites, J. Phys. Chem. C 113 (2009) 13358–13368.
[20] G.G. Qian, J. Zhang, Y.F. Xu, Z.P. Xu, C. Chen, Q. Liu, Reinvestigation of dehydration and dehydroxylation of hydrotalcite-like compounds through combined TG-DTA-MS analyses, J. Phys. Chem. C 114 (2010) 10768–10774.
[21] H.C. Zeng, Z.P. Xu, In situ generation of maximum trivalent cobalt in synthesis of hydrotalcite-like compounds $Mg_xCo^{II}{}_{1-x-y}Co^{III}{}_y(OH)_2(NO_3)_y{\cdot}nH_2O$, Chem. Mater. 12 (2000) 2597–2603.
[22] R.L. Frost, A.W. Musumeci, W.N. Martens, M.O. Adebajo, J. Bouzaid, Raman spectroscopy of hydrotalcites with sulphate, molybdate and chromate in the interlayer, J. Raman Spectrosc. 36 (2005) 925–931.
[23] A. Legrouri, M. Lakraimi, A. Barroug, A. De Roy, J.P. Besse, Preparation of a new stable hybrid material by chloride-2,4-dichlorophenoxyacetate ion exchange into the zinc-aluminium-chloride layered double hydroxide, J. Mater. Chem. 10 (2000) 1007–1011.
[24] T.T. Lim, K.H. Goh, Z. Dong, Application of layered double hydroxides for removal of oxyanions: a review, Water Res. 42 (2008) 1343–1368.
[25] W. Ma, L.L. Xiao, M. Han, Z.H. Cheng, The influence of ferric iron in calcined nano-Mg/Al hydrotalcite on adsorption of Cr (VI) from aqueous solution, J. Hazard. Mater. 186 (2011) 690–698.
[26] P. Refait, S. Loyaux-Lawniczak, J.J. Ehrhardt, P. Lecomte, J.M.R. Genin, Trapping of Cr by formation of ferrihydrite during the reduction of chromate ions by Fe(II)–Fe(III) hydroxysalt green rusts, Environ. Sci. Technol. 34 (2000) 438–443.
[27] G.R. Qian, Y.C. Dai, Y.L. Cao, Y. Chi, Y.F. Xu, J.Z. Zhou, Q. Liu, Z.P. Xu, S.Z. Qiao, Effective removal and fixation of Cr(VI) from aqueous solution with Friedel's salt, J. Hazard. Mater. 170 (2009) 1086–1092.
[28] P.S. Braterman, Z.P. Xu, F. Yarberry, Layered double hydroxides (LDHs), in: S.M. Auerbach, K.A. Carrado, P.K. Dutta (Eds.), Handbook of Layered Materials, Marcel Dekker, New York, 2004, p. 373.
[29] U.A. Birnin-Yauri, F.P. Glasser, Friedel's salt, $Ca_2Al(OH)_6(Cl,OH){\cdot}2H_2O$: its solid solutions and their role in chloride binding, Cem. Concr. Res. 28 (1998) 1713–1723.
[30] J.Z. Zhou, G.R. Qian, Y.L. Cao, P.C. Chui, Y.F. Xu, Q. Liu, Transition of Friedel phase to chromate-AFm phase, Adv. Cem. Res. 20 (2008) 167–173.
[31] C.D. Palmer, Precipitates in a Cr(VI)-contaminated concrete, Environ. Sci. Technol. 34 (2000) 4185–4192.
[32] F.P. Glasser, A. Kindness, S.A. Stronach, Stability and solubility relationships in AFm phases – Part 1. Chloride, sulfate and hydroxide, Cem. Concr. Res. 29 (1999) 861–866.